

Cite this: *Sustainable Food Technol.*,  
2025, 3, 2226

# Characterisation of water-soluble *Nannochloropsis oceanica* protein fractions: physical and functional properties

Thi Phuong Linh Le,<sup>a</sup> Jayani Samarathunga,<sup>a</sup> Katrina Strazdins,<sup>b</sup>  
Jeroen Rens<sup>b</sup> and Benu Adhikari<sup>a</sup>

This study presents a comprehensive physical and functional characterisation of water-soluble protein fractions extracted from defatted *Nannochloropsis oceanica* biomass, including electrostatic surface charge, water-absorption and oil-absorption capacities, foaming, emulsion formation and stability, and thermal behaviour, including denaturation and gelation, benchmarked against two widely used commercial proteins such as milk protein (MP) and soybean protein (SP). The water-soluble *N. oceanica* protein fractions (NP) showed comparable or superior surface charge density, water-absorption capacity, and oil-absorption capacity relative to MP and SP. NP achieved the highest emulsion activity index (131 m<sup>2</sup> g<sup>-1</sup>), the greatest emulsion stability index (121 days), and the most negative zeta potential (−59.3 mV). It also produced the smallest emulsion droplet size among the tested proteins. Its denaturation temperature was 71 °C, indicating good thermal stability. NP formed heat-induced gels at 95 °C with a minimum concentration of 10% (w/w), although the resulting gels were not as firm as those formed by SP. These results indicate that NP possesses emulsifying, thermal, and gelling properties suitable for a range of food applications. Given its sustainable origin and multi-functional performance, NP holds promise as a novel protein ingredient in future foods.

Received 10th July 2025  
Accepted 3rd October 2025

DOI: 10.1039/d5fb00372e

rsc.li/susfoodtech

## Sustainability spotlight

This study supports the transition towards a more sustainable food system by characterising microalgal *Nannochloropsis oceanica* protein, which comes with versatile physical and functional properties. The content aligns with United Nations Sustainable Development Goals (SDGs), particularly zero hunger (SDG 2) and responsible consumption and production (SDG 12). By promoting *Nannochloropsis oceanica* as a less-resource-intensive, high-performance protein alternative, the research contributes to climate action by reducing reliance on land- and water-intensive protein sources (SDG 13). Furthermore, it drives food system innovation (SDG 9), positioning *Nannochloropsis oceanica* protein as a scalable solution for diversifying protein supply chains and shaping a resilient, sustainable future for global nutrition.

## 1 Introduction

The demand for protein-rich foods is surging, driven by global population growth, increasing urbanization, and changing dietary habits. Traditional sources of protein, such as meat and dairy, are facing challenges related to environmental sustainability, animal welfare, and resource scarcity.<sup>1</sup> Consequently, there is increasing interest in exploring alternative protein sources that can meet the nutritional needs of an increasing population while minimizing environmental impact.<sup>2</sup> Microalgae, a diverse group of photosynthetic organisms, have emerged as promising candidates for sustainable protein production. These organisms offer several advantages,

including rapid growth rates, high nutrient content, and the ability to be cultivated in diverse environments.<sup>3</sup> Among the various microalgae species, *Nannochloropsis oceanica* has gained significant attention due to its high biomass yield, favorable fatty acid and amino acid profiles, and potential for large-scale cultivation.<sup>4,5</sup>

Although *N. oceanica* holds promise as a protein-rich food source, its rigid cell wall presents a significant hurdle, particularly in releasing intracellular components such as proteins. Various efforts have been made to develop and optimise the protein extraction process from *N. oceanica* using combinations of physical (e.g., mechanical, thermal, thermo-mechanical processing), chemical (e.g., organic solvents, osmotic shock, acid-alkali treatment), and biological (e.g., enzymatic) pre-treatment methods to produce high-purity protein extracts. However, *N. oceanica* biomass contains a considerable amount of lipids (10–69% in DW), carbohydrates (5–28% in DW),

<sup>a</sup>School of Science, RMIT University, Melbourne, VIC 3083, Australia. E-mail: thi.phuong.linh.le@rmit.edu.au; benu.adhikari@rmit.edu.au

<sup>b</sup>Bega Group, Melbourne, VIC 3008, Australia. E-mail: katrina.strazdins@bega.com.au



polyphenols, pigments, and minerals,<sup>6</sup> which are often co-extracted with proteins during extraction, thereby reducing the overall purity of the extracted protein. Despite previous investigations into proteins extraction from both non-defatted and defatted *Nannochloropsis oceanica* biomass,<sup>7,8</sup> The resulting protein extracts have achieved protein content of only up to 70% in DW. This highlights the need for a procedure that can more effectively remove lipids and other non-protein components to improve protein separation and quality. Additionally, highly purified *N. oceanica* protein extracts remain underutilised in food applications due to limited knowledge of their techno-functional properties. To date, no systematic study has assessed the industrially relevant techno-functionalities of *N. oceanica* protein extracts with high purity or compared them with the functionalities of commonly used food proteins.

The objectives of this study were to characterize the physical properties such as thermal stability and electrostatic surface charge of extracted *Nannochloropsis oceanica* protein with high protein content (up to 80% in DW), and to compare its functional properties including water-absorption and oil absorption capacities, emulsion droplet size and charge density, emulsion activity and stability indices, and gelation with those of two widely used food proteins, namely milk and soybean protein. These physicochemical and functional properties play a critical role in determining a protein's suitability for various food applications, such as emulsified products, plant-based dairy alternatives, and protein-enriched gels. Understanding how *N. oceanica* protein performs in these contexts is essential for evaluating its potential as a sustainable alternative to conventional food proteins.

## 2 Materials and methods

### 2.1 Materials

The freeze-dried *Nannochloropsis oceanica* (*N. oceanica*) powder was donated by Qponics Limited (Brisbane, Queensland, Australia). Milk protein (MP, protein content: 82.4% in dry weight (DW)) was donated by Tatura Milk Industries Limited (Tatura, Victoria, Australia) and soybean protein (SP, protein content: 88.2% in DW) was purchased from Bulk Nutrients (Grove, Tasmania, Australia). These two commercially available proteins served as benchmarks for comparing the physical and functional properties of the protein extracted from *N. oceanica*. Sunflower oil was purchased from a local supermarket to prepare oil-in-water emulsions. Analytical grade acetone was purchased from ChemSupply Australia Pty. Ltd (Australia). All other chemicals used in this study were purchased from Sigma-Aldrich Australia (Sydney, New South Wales, Australia) and were used as received. The Pierce™ Bradford Protein Assay Kit and bovine serum albumin (BSA) were of analytical grade and purchased from Thermo Fisher Scientific (USA).

### 2.2 Extraction of protein

Protein was extracted from the freeze-dried *N. oceanica* biomass using a procedure previously reported by our group.<sup>9</sup> Briefly, the biomass was pulverised using a laboratory blender (8011ES, John Morris Group, Australia). The ground biomass was

defatted through two extraction cycles of 2 h each using acetone at a biomass-to-acetone ratio of 1 : 5 (w/v). The defatted biomass was then air-dried in a fume hood for 72 h to remove residual acetone. This dried biomass was soaked in Milli-Q water adjusted to pH 12.0 with 1.0 M NaOH, at a biomass-to-buffer ratio of 1 : 20 (w/v), and agitated at 700 rpm for 5 h. The mixture was then centrifuged at 10 000×g for 30 min using a centrifuge (Sorvall LYNX 6000, Thermo Fisher Scientific, USA). The supernatant was collected, and its pH was adjusted to 2.0 – the isoelectric point of *N. oceanica* protein – using 1.0 M HCl to induce protein precipitation.

The mixture was stored at 4 °C for 16 h to allow complete precipitation, after which the precipitated protein was collected by centrifugation at 10 000×g for 30 min. The pellet was redispersed in Milli-Q water and neutralised using 1.0 M NaOH. Finally, the *N. oceanica* protein (NP) was obtained by freeze-drying at –40 °C and 10 Pa using a freeze dryer (VaCo 10, Zirbus Technology GmbH, Germany). The freeze-dried NP was vacuum-sealed and stored at –20 °C until further use. The protein contents of the NP and benchmark samples were determined using Kjeldahl method (AOAC Method 991.20).<sup>10</sup>

### 2.3 Determination surface charge

For surface charge (zeta potential) measurements, the protein suspensions were prepared by dispersing 50 mg of protein powder in 10 mL of Milli-Q water, followed by stirring for 1 hour to ensure complete hydration. The pH of the dispersions was adjusted over a range of 2.0 to 12.0, in one-unit increments, using 0.1 M HCl or 0.1 M NaOH. The samples were agitated at room temperature (25 ± 2 °C) for 2 h, stored at 4 °C overnight, and then centrifuged at 10 000×g for 30 min. The supernatant was collected, allowed to return to room temperature, and transferred into folded capillary cells. Zeta potential was measured as a function of pH using a dynamic light scattering-based instrument (Zetasizer ZS-90, Malvern Instruments, Worcestershire, UK) at 25 °C.<sup>11</sup>

### 2.4 Determination of solubility

The solubility of NP was measured according to Zhang *et al.*,<sup>13</sup> with some modifications. Briefly, 100 mg of NP powder was mixed with 10 mL of Milli-Q water and stirred for 1 hour to ensure complete hydration. The pH of the resulting dispersions was adjusted from 2.0 to 12.0, in one-unit increments, using 0.1 M HCl or 0.1 M NaOH. Each dispersion was agitated at room temperature (25 ± 2 °C) for 2 hours, stored at 4 °C overnight, and then centrifuged at 10 000×g for 30 minutes. The solubilised protein content in the collected supernatants was determined using the Pierce™ Bradford Protein Assay Kit. Bovine serum albumin (BSA) was used to generate a standard curve. Protein solubility (%) was calculated as the ratio of protein content in the supernatant to the total protein content in the initial powder.

### 2.5 Determination of water-absorption and oil-absorption capacities

The water-absorption capacity (WAC) and oil-absorption capacity (OAC) were determined according to Tomotake



*et al.*<sup>12</sup> with minor modifications. One gram of protein was dissolved into 10 mL of Milli-Q water in a pre-weighed centrifuge tube. The pH of the samples was adjusted to 7.0 using 0.1 M HCl or NaOH as required. The mixture was vortexed for 1 min, allowed to stand for 30 min at ambient temperature, and then centrifuged at 10 000×*g* for 30 min. The supernatant was decanted carefully, and the tube with sediment was weighed again. The water-absorption capacity was expressed as grams of water held by 1 g of extracted protein using eqn (1).

$$\begin{aligned} \text{Water-absorption capacity (g of water per g of protein)} \\ = \frac{W_2 - W_1}{W_0} \times 100 \end{aligned} \quad (1)$$

where,  $W_0$  = weight of dry protein extract (g);  $W_1$  = weight of the centrifuge tubes and dry protein extract (g);  $W_2$  = weight of the centrifuge tubes and pellets (g).

The oil-absorption capacity was determined using a similar procedure using 1 g of protein and 10 mL of sunflower oil. The oil-absorption capacity was expressed as grams of oil absorbed by 1 g of extracted protein using eqn (2).

$$\begin{aligned} \text{Oil-absorption capacity (g of oil per g of protein)} \\ = \frac{W_2 - W_1}{W_0} \times 100 \end{aligned} \quad (2)$$

where,  $W_0$  = weight of dry protein extract (g);  $W_1$  = weight of the centrifuge tubes and dry protein extract (g);  $W_2$  = weight of the centrifuge tubes and pellets (g).

## 2.6 Determination of foaming capacity and foam stability

For these tests, protein suspensions of 2% (w/v) in Milli-Q water were prepared, and the pH of the suspensions was adjusted to 7.0 using 0.1 M HCl or NaOH as required. The suspensions were then whipped in a high-speed Ultra-Turrax homogeniser (Ika, T25, Germany) for 2 min at 15 000 rpm. The foaming capacity and foam stability were evaluated by measuring the foam volume after 5, 10, 15, 30, and 60 min of samples resting at room temperature. The foaming capacity and foam stability were calculated by using eqn (3) and (4), respectively.

$$\text{Foaming capacity (\%)} = \frac{FV}{V_{\text{initial}}} \times 100 \quad (3)$$

$$\text{Foam stability (\%)} = \frac{FV_{\text{time } t}}{FV} \times 100 \quad (4)$$

where FV = foam volume (mL);  $V_{\text{initial}}$  = volume of the solution before homogenisation (mL);  $FV_{\text{time } t}$  = remaining foam volume after resting time interval  $t$  (mL).

## 2.7 Emulsifying activity and emulsion stability indices

**2.7.1 Preparation of emulsions.** Oil-in-water (O/W) emulsions were prepared according to Zhang *et al.*<sup>13</sup> with some modifications. Briefly, the protein solutions of NP, MP, and SP were prepared by dissolving them in Milli-Q water at varying concentrations (1–3%, w/v). They were stirred for 30 min to ensure complete dissolution. The pH of the solutions was adjusted to 7.0 using 0.1 M HCl or NaOH as required. The

emulsions with sunflower oil (10% v/v) were prepared using NP, MP, and SP solutions as emulsifiers. The suspensions were homogenised by an Ultra-Turrax homogeniser at 15 000 rpm for 2 min to make coarse emulsions. These coarse emulsions were homogenised using a microfluidiser (M-110L, Microfluidics International Corporation, USA) at 62 MPa using 3 passes to obtain fine emulsions. During emulsion preparation, the homogenization chamber and microfluidiser coils were immersed in an ice bath to maintain the processing temperature below 20 °C. The emulsions were stored at 4 °C for further analysis. The emulsions were brought to ambient temperature by allowing them to stand for 2 h before they were analysed.

**2.7.2 Determination of emulsifying activity and emulsion stability indices.** The emulsifying activity index (EAI) of extracted protein and the emulsion stability index (ESI) of protein emulsions were determined by using a turbidimetric method.<sup>13,14</sup> Freshly prepared emulsions were diluted 100 times with 0.1% (w/v) sodium dodecyl sulphate (SDS) and mixed for 1 minute using a vortex mixer. The absorbance of these diluted emulsions in quartz cuvettes with a path length of 0.01 m was measured at 500 nm wavelength using a UV/Vis Spectrophotometer (Lambda 365, PerkinElmer Inc., USA). The turbidity of the emulsion will be calculated using eqn (5).

$$T = 2.303 \times \frac{A}{L} \times D \quad (5)$$

where  $T$  = the turbidity of emulsion in  $\text{m}^{-1}$ ;  $A$  = the absorbance (dimensionless);  $D$  = the dilution factor (dimensionless), which is 100;  $L$  = the light path length of the cuvette, which is 0.01 m.

The emulsifying activity index (EAI, expressed in  $\text{m}^2 \text{g}^{-1}$ ) and emulsion stability index (ESI, expressed in min) were calculated using eqn (6) and (7), respectively.

$$\text{EAI} = \frac{2 \times T_0}{\emptyset \times C \times 1000} \quad (6)$$

$$\text{ESI} = \frac{T_0}{T_0 - T} \times t \quad (7)$$

where,  $T_0$  = the turbidity of fresh emulsion in  $\text{m}^{-1}$ ;  $\emptyset$  = the oil volume fraction (dimensionless), which is 0.1;  $C$  = the concentration of protein in the dispersion ( $\text{mg mL}^{-1}$ );  $t$  = the time interval (24 h);  $T$  = the turbidity of the emulsion after interval storage.

**2.7.3 Determination of particle size and zeta potential of emulsions.** The  $Z$ -average diameter and zeta potential of droplets in a protein-stabilised O/W emulsion were determined using a Zetasizer within 24 h of emulsion preparation. The emulsions were diluted 100 times with Milli-Q water before these measurements to avoid multiple scattering effects.

## 2.8 Thermal analysis of protein

Thermal characteristics of NP were determined using a differential scanning calorimeter (DSC, Q2000, TA Instruments, USA). Two milligrams of protein samples were weighed in an aluminium Tzero pan. The pan was hermetically sealed and heated from 25 to 180 °C under 50  $\text{mL min}^{-1}$  nitrogen gas purge



at a  $5\text{ }^{\circ}\text{C min}^{-1}$  heating rate. An empty aluminium pan was used as the reference. The onset ( $T_m$ ) and peak ( $T_d$ ) denaturation temperatures and enthalpy of denaturation ( $\Delta H$ ) were determined from the thermograms using the associated software (TA Universal Analysis 2000).

## 2.9 Gelation

**2.9.1 The least gelation concentration.** The least gelation concentration (LGC) of the tested proteins was measured according to Ma *et al.*<sup>15</sup> with some modifications. Three protein (NP, MP and SP) solutions with the concentrations of 2–10% (w/w) were prepared at pH 7.0. Subsequently, 1 mL of each protein solution was transferred into an Eppendorf tube and heated for 1 h in a dry block heater (Ratek, Australia) at  $95\text{ }^{\circ}\text{C}$ . After heating, the samples were cooled down to  $25\text{ }^{\circ}\text{C}$  using water for 2 min and subsequently transferred to a refrigerator at  $4\text{ }^{\circ}\text{C}$  for overnight. After this, the LGC was analysed, and the lowest concentration of protein required to form the gel was determined.

**2.9.2 Gelation kinetics.** Gelation kinetics was determined using a stress-controlled rheometer (AR2000ex, TA Instruments Ltd, UK). A Peltier plate system with a cone geometry was used. The diameter, cone angle and the gap were 60 mm,  $2^{\circ}$  and 52  $\mu\text{m}$ , respectively. The temperature of the sample increased from  $25$  to  $95\text{ }^{\circ}\text{C}$  with a heating rate of  $2\text{ }^{\circ}\text{C min}^{-1}$ , then cooled back to  $25\text{ }^{\circ}\text{C}$  with a cooling rate of  $5\text{ }^{\circ}\text{C min}^{-1}$ . The storage ( $G'$ ) and loss ( $G''$ ) moduli were measured during both heating and cooling steps as a function of time. At the end of the measurement, a strain sweep was performed from 0.1% to 100% at  $25\text{ }^{\circ}\text{C}$ . Samples were covered with a thin layer of paraffin oil to prevent evaporation.<sup>16</sup>

## 2.9.3 Statistical analysis

Statistical analyses were performed using IBM's SPSS Statistics 28 (IBM, USA). All experimental measurements were conducted at least in triplicate. The results are reported as mean value  $\pm$  standard deviation. The analysis of variance (ANOVA) was performed to determine the significant difference between any two mean values. The Duncan test was implemented on the data sets using a 95% significance level ( $P < 0.05$ ).

## 3 Results and discussion

The *Nannochloropsis oceanica* protein extract (NP), derived from acetone-defatted biomass, demonstrated a high protein content of 86.4% [ $N \times 6.25$ ] on a dry weight basis. To assess its potential for food applications, the physicochemical properties of NP were characterised, with particular emphasis on thermal stability and electrostatic surface charge. Furthermore, its functional attributes including water and oil absorption capacities, emulsion droplet size and charge density, emulsion activity and stability indices, and gelation behaviour were systematically compared to those of milk (MP) and soybean (SP) proteins, which contained 82.4% [ $N \times 6.38$ ] and 88.2% [ $N \times 5.71$ ] protein (dry weight), respectively.

## 3.1 Surface charge

The variation in surface charge (zeta potential) of protein in biomass and the *N. oceanica* protein extracts (NP) in the pH range of 2.0–12.0 is shown in Fig. 1. Overall, at most pH values, the magnitude, or the absolute value, of the surface charge of the protein in NP was higher than that of the biomass. The maximum negative charge was observed at pH 12.0 due to increased exposure of anionic groups on the protein surface. The magnitude of the surface charge of both proteins in biomass and NP decreased as pH decreased. However, only the surface charge of protein in biomass reached zero (neutral) at pH 2.0, while the surface charge of protein in NP was still negative at this pH value. This variation implied that the extraction procedure modulated surface charge properties, potentially by removing associated non-protein constituents—such as lipids, carbohydrates, or polyphenols—that might contribute to charge distribution. In the isolated protein extracts, the absence of these components likely altered intermolecular interactions and electrostatic behaviour. It is commonly accepted that a magnitude of zeta potential higher than 30.0 mV is desired for electrostatic stabilisation of the suspended protein systems. The zeta potential of NP solutions showed consistently negative values in the entire pH range tested (2.0–12.0), with values spanning from  $-7.6$  to  $-47.2$  mV. This trend closely resembles the zeta potential behaviour observed in other algal proteins (*e.g.* *Arthrospira platensis* (*Spirulina*), *Phaeodactylum tricornutum*, *Chlorella*) which typically display mildly positive values at pH 2.0, decrease toward zero near pH 3.0, and become increasingly negative with further increase of pH.<sup>17–22</sup> However, this pH-versus zeta potential pattern of the algal proteins differs with that observed in plant and dairy protein, which generally display positive values at acidic pH (*e.g.*, pH 3.0), decrease toward zero near their isoelectric points (typically between pH 4.0 and 5.0), and then shift to increasingly negative values as the increased from 5.0 to 11.0.<sup>23</sup> The distinct zeta potential profile of NP proteins could be

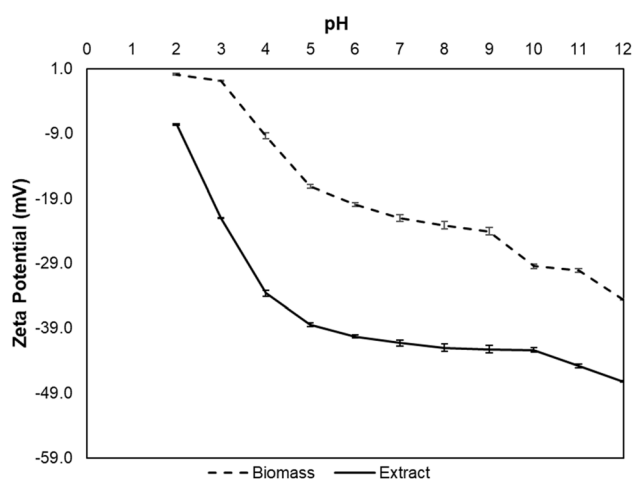


Fig. 1 The variation of electrostatic charge density (zeta potential) of *Nannochloropsis oceanica* protein in biomass and its protein extract as a function of pH at room temperature ( $25 \pm 2\text{ }^{\circ}\text{C}$ ).



attributed to their high content of acidic amino acids. Aspartic acid and glutamic acid together constitute approximately 8–12% of the total amino acid content in most microalgae, contributing to the overall negative surface charge across a wide pH range.<sup>24</sup> Notably, within the pH range commonly encountered in food systems (pH 4.0–9.0), NP protein solutions remained stable as indicated by strongly negative zeta potential values (−33.6 to −47.2 mV). Thus, NP proteins had greater electrostatic stability compared to plant and dairy milk proteins in the wider pH range.<sup>17,18,23,25</sup> This suggests that the NP would be stable in the suspension systems (*i.e.*, protein-rich foods) in this pH range.

### 3.2 Solubility

The solubility of NP across the pH range of 2.0–12.0 is shown in Fig. 2. The lowest solubility was observed at pH 2.0, reaching  $5.15\% \pm 0.2$ , which is close to the isoelectric point (pI) of *Nannochloropsis oceanica* protein, reported at pH 2.0.<sup>9</sup> A rapid increase in solubility occurred between pH 2.0 and 4.0, reaching approximately  $81.8\% \pm 0.8$ , significantly outperforming conventional plant and dairy proteins in the acidic pH range. Unlike many proteins that show only gradual increases beyond their pI, NP maintained consistently high solubility ( $\sim 83\%$ ) from pH 5.0 to 7.0 and increased further to above 90% from pH 8.0 to 12.0. This trend aligns with the zeta potential values of NP, which remained strongly negative (−38.6 to −47.2 mV) across pH 5.0–12.0, suggesting that increased surface charge may enhance solubility by promoting stronger interactions between solute and solvent molecules.<sup>26</sup> Additionally, NP in this study demonstrated superior solubility compared to water-soluble protein extracts from *N. oceanica* ( $\geq 79\%$ ) (in previous study), *Chlorella sorokiniana* ( $\geq 68\%$ ), and *Phaeodactylum tricorutum* ( $\geq 50\%$ ) within the pH range of 6.0 to 12.0,<sup>27</sup> and was comparable to the solubility of *Spirulina platensis* protein, which reached approximately 98% at pH 8.0–9.0.<sup>28,29</sup> This favorable solubility profile highlights the potential of NP as a functional protein ingredient for a wide range of applications,

particularly in acidified food systems with target pH values of 7.0 or lower.

### 3.3 Water-absorption and oil-absorption capacities

The water-absorption capacity (WAC) is described as a protein's ability to hold or absorb water. The WAC of NP was significantly lower than that of soybean protein (SP) but was similar to milk protein (MP) (Fig. 3). The ability of protein extracts to bind water is influenced by factors such as the molecular structure of the protein and the distribution of hydrophilic and hydrophobic amino acids of the protein.<sup>8</sup> A higher WAC in proteins might be associated with low solubility. It could be explained that proteins exhibiting high solubility generally exhibit an increased presence of hydrophilic regions, which enhances their aqueous dispersibility while limiting their propensity to aggregate into structures capable of immobilising water.<sup>30</sup> It was reported that *N. oceanica* protein exhibited the highest WAC ( $2.9 \pm 0.1$  g water per g protein) compared to *Chlorella pyrenoidosa* protein ( $2.0 \pm 0.1$  g water per g protein) and *Arthrospira platensis* ( $2.8 \pm 0.0$  g water per g protein).<sup>8</sup> The NP in this work had a WAC of  $2.6 \pm 0.3$  g water per g protein, which is close to the value reported by Chen *et al.*<sup>8</sup> The differences in WAC among NP, MP, and SP could be attributed to variations in protein–water interactions, likely caused by differences in the polar amino acid composition of these proteins.<sup>8</sup>

The oil-absorption capacity (OAC) is defined as the amount of oil that can be absorbed per unit protein weight. OAC is an important property of proteins as it influences the texture and stability of food products. The OAC of NP was the highest, followed by MP and SP. SP had the lowest OAC, indicating that it was more hydrophilic in nature. NP had the lowest WAC but the highest OAC, indicating a higher proportion of the non-polar amino acids such as valine, leucine, proline, or isoleucine, which were found in a considerable amount in *Nannochloropsis* spp.<sup>31</sup> The higher concentration of these non-polar amino acids meant that NP is expected to have higher number of lipophilic

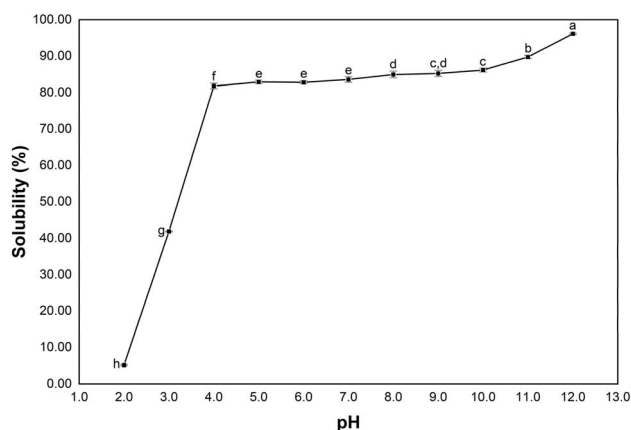


Fig. 2 The solubility of *Nannochloropsis oceanica* protein extract as a function of pH at room temperature ( $25 \pm 2$  °C). The bars with different letters are significantly different ( $p < 0.05$ ).

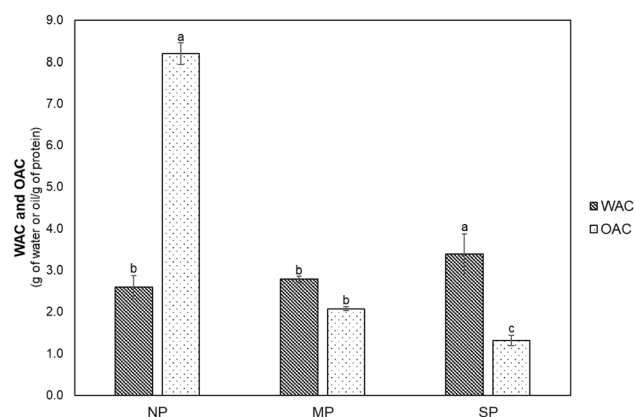


Fig. 3 Comparison of water-absorption capacity (WAC) and oil-absorption capacity (OAC) of *Nannochloropsis oceanica* protein extracts (NP), milk protein (MP), and soybean protein (SP) that were measured at pH 7.0 and room temperature ( $25 \pm 2$  °C). The bars with different letters are significantly different ( $p < 0.05$ ).



sites in its structure than in the MP and SP.<sup>32</sup> The OAC of NP was comparable to other microalgae proteins, e.g., as *Arthrospira platensis* protein with OAC ranging from 5.8–8.4 g oil per g protein, but it was considerably higher than that of *Chlorella pyrenoidosa* protein (6.7 g oil per g protein) or *Isochrysis galbana* (3.16 g oil per g protein).<sup>8,29,33,34</sup> Thus, the strong oleophilic nature of NP could be useful in oil-rich foods.

### 3.4 Foaming capacity and foam stability

Protein foaming properties, including foaming capacity and foam stability, are commonly associated with a protein's ability to form and stabilise foams by rapidly adsorbing at the air–water interface. Foaming capacity refers to the volume of foam produced when a protein solution is whipped, which reflects how effectively the protein can stabilise newly formed air bubbles.<sup>35</sup> The foaming capacities of NP, MP, and SP are presented in Table 1. The data show that NP exhibited higher foaming capacity than MP and SP. These results are consistent with previous findings showing that microalgae-derived soluble proteins exhibit superior foaming capacity compared to whey and soybean proteins within the pH range of 5–7.<sup>36,37</sup> Notably, NP demonstrated comparable or even greater foaming capacity at neutral pH than proteins extracted from other microalgae, such as *Arthrospira platensis* (135%), and *Chlorella pyrenoidosa* (130%),<sup>8</sup> *Arthrospira platensis* (150%),<sup>33</sup> and *Spirulina platensis* (218%).<sup>34</sup> The higher foaming capacity of NP at neutral pH could be attributed to its greater protein solubility, which enhances molecular flexibility and accelerates diffusion to the air–water interface, enabling proteins to more effectively encapsulate air bubbles.<sup>38</sup>

Foam stability refers to the ability of a foam to retain its volume over time, typically measured as the percentage of the original foam volume remaining after a given period.<sup>35</sup> NP demonstrated greater foam stability compared to MP and SP. As shown in Fig. 4, NP foams remained highly stable and exhibited a trend similar to MP over the 60 minutes testing period. The foam volume from NP decreased only slightly to approximately 90.9% after 60 min, whereas the foam from SP dropped significantly to 67.5%, indicating a weak interfacial film formed by SP. Foam stability is influenced by multiple factors, including protein concentration, molecular structure, interfacial film properties (e.g., interfacial cohesiveness, dilatational viscosity, and dilatational elasticity), pH, and temperature.<sup>39</sup> NP exhibited a strong negative surface charge at pH 7.0, which induced electrostatic repulsion between protein molecules at the interface. This repulsion minimized aggregation and

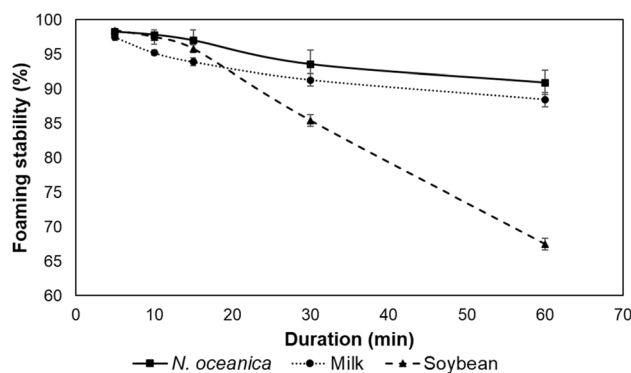


Fig. 4 Foaming capacity and stability of *Nannochloropsis oceanica* protein extracts compared with milk and soybean protein at pH 7.0 and ambient temperature ( $25 \pm 2$  °C).

promoted the formation of a cohesive interfacial film, aiding in the prolonged retention of air bubbles.<sup>38</sup> Additionally, the high solubility of NP at pH 7.0 contributed to foam stability by increasing protein availability at the air–water interface, facilitating the formation of a continuous, resilient film around air bubbles, and preventing bubble coalescence and foam collapse over time.<sup>40–42</sup> Under the current experimental conditions – 2% protein concentration, pH 7.0, and room temperature – NP appeared to be the most suited for stable foam formation.

### 3.5 Oil-in-water (O/W) emulsions

#### 3.5.1 Zeta potential and average diameters of oil droplets.

In oil-in-water emulsions, oil droplet size and zeta potential are critical parameters influencing their stability.<sup>43</sup> It is essential for emulsions to have sufficiently small droplet/particle size ( $\leq 1$   $\mu\text{m}$ ) to enable them resist gravitational separation and thereby preventing destabilization of oil-in-water (O/W) emulsions.<sup>44,45</sup> Three emulsions (NP-1%, NP-2%, and NP-3%) were prepared using NP at concentrations of 1%, 2%, and 3% (w/w), respectively, under a homogenisation pressure of 62 MPa. All emulsions exhibited mean droplet sizes below 1  $\mu\text{m}$ , indicating a stable emulsification system. An increase in protein concentration from 1% to 3% resulted in smaller droplet formation. The average droplet diameter in NP-1% emulsions was  $637.2 \pm 2.7$  nm, which was significantly larger than that of NP-2% and NP-3% emulsions (Fig. 5A). The emulsifying and interfacial properties of proteins are highly dependent on concentration. Increasing protein content in the emulsion system can enhance surface protein coverage and reduce interfacial tension between oil and water by promoting the formation of a protein-rich interfacial film on oil droplets, thereby facilitating the formation of smaller, more stable droplets.<sup>46,47</sup> The NP-1% emulsion was then compared with emulsions stabilised by MP-1% and SP-1%, each containing 1% (w/w) protein, to assess their relative performance. Previous studies have shown that milk proteins are generally more effective at creating and stabilizing smaller oil droplets in emulsions compared to plant proteins such as faba bean, lentil, and pea.<sup>48</sup> In this study, the NP-1% emulsion showed an average droplet diameter comparable to

Table 1 Foaming capacity of *Nannochloropsis oceanica* protein extracts compared with milk and soybean protein at pH 7.0 and ambient temperature ( $25 \pm 2$  °C). The different letters indicate a significant difference ( $p < 0.05$ )

Protein	Foaming capacity (%)
<i>N. oceanica</i>	$216.2 \pm 0.3^a$
Milk	$182.9 \pm 4.1^b$
Soybean	$191.59 \pm 1.2^b$



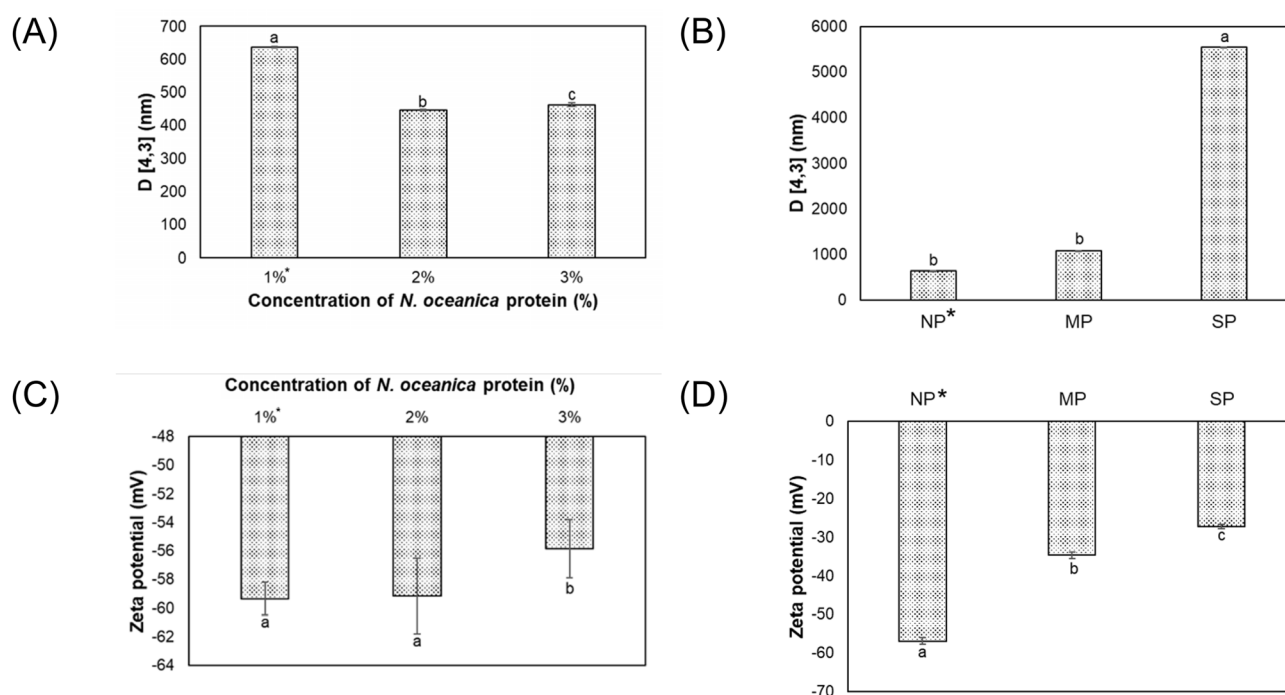


Fig. 5 Average size (diameter, nm) (A and B) and zeta potential (mV) (C and D) of oil droplets in emulsion stabilised by *Nannochloropsis oceanica* protein extract at different emulsifier concentrations (A and C); and stabilised by different proteins such as *N. oceanica* protein (NP), milk protein (MP) and soybean protein (SP) at 1% of emulsifier concentration (B and D) at pH 7.0 and ambient temperature ( $25 \pm 2$  °C). The bars with different letters were significantly different ( $p < 0.05$ ). (\*) The data of NP-1% emulsion in Fig. 5A and C is repeated in NP emulsions in Fig. 5B and D for comparison.

that of the MP-1% emulsion, and significantly smaller than the droplet size observed in the SP-1% emulsion (Fig. 5B). Notably, the SP emulsion exhibited a significantly larger droplet size (5.55  $\mu\text{m}$ ), which could be attributed to its lower emulsifying activity (EAI) and emulsion stability (ESI) indices. These observations suggest that the emulsifying capacity of NP at 1% concentration exhibits similar effectiveness as that of MP, while outperforming SP under identical formulation conditions.

In oil-in-water (O/W) emulsions, proteins act as interfacial barriers that prevent droplet agglomeration. Emulsion stability is largely governed by electrostatic repulsion between these protein-coated droplets. The magnitude of this repulsion is reflected in the zeta potential, which measures surface charge. A higher absolute zeta potential indicates stronger electrostatic repulsion and, consequently, greater emulsion stability. As a general guideline, emulsions with zeta potential values exceeding  $\pm 30$  mV are considered electrostatically stable, as the repulsive forces are sufficient to prevent droplet coalescence and phase separation.<sup>49</sup>

The zeta potential of O/W emulsion droplets stabilised by NP was measured at three of its concentrations (1%, 2%, and 3%, w/w). All three emulsions showed strong electrostatic stabilisation, with zeta potential values ranging from  $-55.9$  to  $-59.3$  mV. No significant difference was observed between the 1% and 2% NP emulsions; however, the 3% NP emulsion exhibited a slightly less negative zeta potential. This reduction in magnitude may be due to increased protein adsorption at higher concentrations, which can lead to more complete

surface coverage and partial charge screening at the oil–water interface. Compared to emulsions stabilised by MP and SP under the same conditions, NP-stabilised emulsions showed substantially higher zeta potential values ( $-59.3$  mV), indicating stronger electrostatic repulsion and greater emulsion stability.

**3.5.2 Emulsion activity and emulsion stability indices.** The effectiveness of a protein as an emulsifier is typically assessed by its ability to form and stabilise emulsions. EAI reflects how efficiently a protein can adsorb to the oil–water interface to form a stabilising interfacial layer and is measured based on the turbidity of the emulsion. ESI indicates the protein's ability to prevent droplet agglomeration, coalescence, and phase separation over time.

The EAI and ESI of NP-stabilised emulsions at 1–3% (w/w) concentrations were measured 24 h after emulsion formation at neutral pH. As shown in Fig. 6A and B, NP-1% emulsions exhibited significantly higher EAI and ESI values compared to NP-2% and NP-3% under the same conditions. The EAI of NP was found to increase as its concentration decreased, due to the inverse relationship between protein concentration and the EAI calculation. Additionally, the lower EAI and ESI values observed at higher NP concentrations corresponded to larger droplet sizes, a trend commonly associated with weaker emulsion performance.<sup>50</sup> However, the droplets in NP-2% and NP-3% emulsions exhibited smaller average sizes compared to those in NP-1% emulsions, which appeared to contradict the EAI and ESI results. This suggests that droplet size alone was not the



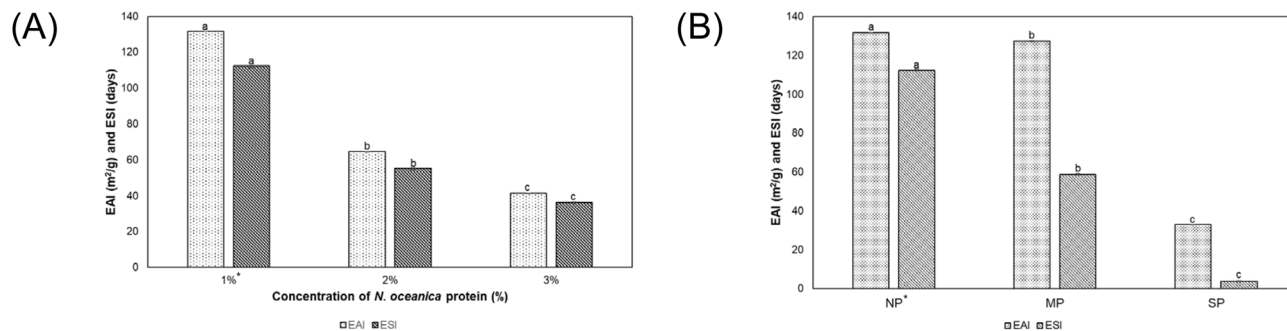


Fig. 6 (A) Emulsifying activity index (EAI) ( $\text{m}^2 \text{g}^{-1}$ ) and emulsifying stability index (ESI) (days) values of emulsion prepared by *N. oceanica* protein extracts at 1 to 3% concentration; and (B) comparison of EAI and ESI values of emulsion prepared by *N. oceanica* protein (NP) with different proteins as milk protein (MP) and soybean protein (SP) at 1% of emulsifier concentration at pH 7.0 and ambient temperature ( $25 \pm 2$  °C). The bars with different letters were significantly different ( $p < 0.05$ ). (\*) The data of NP-1% emulsion in Fig. 6A is repeated in NP emulsions in Fig. 6B for comparison.

primary factor governing emulsion stability. Instead, stability may have been more influenced by the surface charge of the emulsion droplets or by differences in density between the dispersed and continuous phases.<sup>11,32,50</sup> Although NP-2% and NP-3% emulsions had smaller average droplet sizes, their span values-indicating broader particle size distributions-were higher than those of NP-1% (data not shown). This indicated that the emulsions were less homogeneous, which may have increased the likelihood of droplet aggregation and coalescence over time. As a result, the EAI and ESI values of NP-2% and NP-3% emulsions were lower than those of NP-1% emulsions.

The EAI and ESI of NP-1% were compared with those of MP-1% and SP-1% (Fig. 6B). The EAI and ESI values for these emulsions ranged from 33 to 132  $\text{m}^2 \text{g}^{-1}$  and 4 to 121 days, respectively. NP-1% exhibited the highest EAI and ESI values among these protein-stabilised emulsions. These results particularly the exceptionally high ESI of NP-1%, indicate that it has immense potential as an emulsifier for O/W emulsions.

### 3.6 Thermal properties of NP

Thermal denaturation temperature ( $T_d$ ) and enthalpy change ( $\Delta H$ ) are key indicators of a protein's thermal behaviour.  $T_d$  reflects the protein's resistance to heat-induced structural changes, while  $\Delta H$  represents the amount of heat required to induce denaturation. The thermogram of *N. oceanica* protein extracts showed two thermal transitions in the range of 25–180 °C (Fig. 7). The first transition, observed at 71.0 °C, corresponded to protein denaturation, while the second transition at 144.9 °C was attributed to thermal decomposition. The onset denaturation temperature ( $T_o$ ), peak denaturation temperature ( $T_d$ ), and enthalpy of transition ( $\Delta H$ ) were 68.4 °C, 71.0 °C, and 1.704  $\text{J g}^{-1}$ , respectively. *N. oceanica* protein exhibited greater thermal stability than *Arthrospira platensis* and *Chlorella pyrenoidosa*, as reflected in its higher onset denaturation temperature. The  $T_o$  values for *A. platensis* and *C. pyrenoidosa* proteins were 63.9 °C and 47.9 °C, respectively, indicating lower thermal stability. Notably, both *A. platensis* and *C. pyrenoidosa* protein extracts

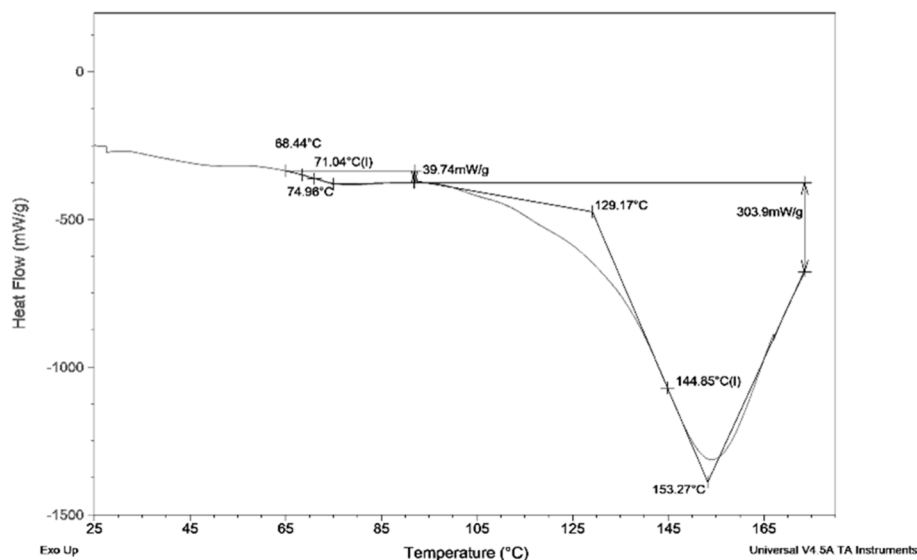


Fig. 7 Differential scanning calorimetry heating thermogram of *Nannochloropsis oceanica* protein showing the denaturation temperature.



showed a single endothermic peak. The  $T_d$  of *C. pyrenoidosa* was approximately 80.8 °C, which was higher than those of *A. platensis* (~76.2 °C) and *N. oceanica* (71.0 °C).<sup>8</sup> In this study, the  $T_d$  of NP was lower than that of SP (87.4 °C), but higher than that of MP (64.4 °C). This observation is consistent with previous studies comparing the denaturation temperature of NP with other protein sources. Specifically, the  $T_d$  of NP was slightly lower than that of SP (75–90 °C) and hemp seed protein (78 °C), yet higher than that of whey protein (65 °C),<sup>51–53</sup> indicating that it has intermediate thermal stability among the aforementioned protein sources. These differences in denaturation temperature are expected, since they are influenced by several factors, including the protein source, extraction method, degree of purity, moisture content, and the presence of non-protein components.<sup>32</sup> On the other hand, the denaturation enthalpy ( $\Delta H$ ) of NP in this study was lower than that of MP (2.339 J g<sup>-1</sup>) and SP (7.485 J g<sup>-1</sup>). It was also lower than values reported for other microalgal protein extracts, such as *Spirulina* (17.4 J g<sup>-1</sup>) and *Chlorella vulgaris* (2.74–5.07 J g<sup>-1</sup>).<sup>54,55</sup> However, the enthalpy change ( $\Delta H$ ) is typically normalized to the total molar concentration of protein, and its magnitude tends to scale proportionally with molecular size and structural complexity. Consequently, proteins with higher molecular weights generally exhibit greater  $\Delta H$  values due to the higher energy required to disrupt their conformational integrity. Previous studies have reported that *N. oceanica* proteins range in size from 1.6 to 20 kDa, which is smaller than the molecular weights of proteins from other common microalgae, such as *Spirulina* (up to 150 kDa) and *Chlorella* spp. (up to 120 kDa),<sup>8,56</sup> as well as typical plant and dairy proteins like soybean (300–380 kDa) and milk proteins (20–25 kDa).<sup>57</sup> This difference in molecular weight likely explains why *N. oceanica* proteins required less energy to unfold during thermal denaturation.

### 3.7 Gelation

**3.7.1 The least gelation concentration.** The ability of proteins to form gels is a desirable property in many food applications. Proteins such as whey, casein, soy, and pea are well known for their effective gel-forming abilities.<sup>58</sup> This study investigated the gel-forming capability of NP and compared it with that of MP and SP. To assess gelation propensity, the least

gelation concentration (LGC)-the minimum protein concentration required to form a gel-was first determined, as described in Section 2.8.1.

As shown in Fig. 8, a minimum protein concentration was required to form a gelled matrix with sufficient structural integrity to remain intact when the tube was inverted. The LGC values for the three proteins (NP, MP, and SP) ranged from 2% to 10% (w/w). The lowest LGC was observed for SP, which formed a gel at just 2% (w/w), while NP required a minimum of 10% (w/w) protein to form a gel. Compared to the minimum heat-induced gelling concentrations in water reported for other algal proteins at similar pH levels, NP required a comparable or higher concentration to initiate gelation under similar conditions. For example, *Chlorella* spp. formed heat-induced gels at 9.9–14% (w/w), *Schizochytrium* sp. at 5–13% (w/w), and *Spirulina* at 12–15% (w/w).<sup>58–60</sup> However, compared to legume-derived proteins such as yellow pea (LGC at 12.5%, w/w), lentil, and faba bean (both with LGC at 10%, w/w), NP showed a lower LGC, suggesting superior gelling efficiency relative to these pulse-based proteins.<sup>61</sup> In contrast, MP did not form a gel even at the highest tested concentration of 10% (w/w) at pH 7.0. This lack of gelation could be attributed to the high proportion of micellar caseins present in the MP samples. Previous studies have shown that heat-induced gelation of casein micelles can occur across a broad concentration range (2.5–16%, w/w), but typically within a lower pH range of 5.2 to 6.7. At comparatively higher protein concentrations (e.g., 16% w/w) and elevated temperatures (e.g., 90 °C), casein micelle suspensions have been shown to form self-supporting gels at pH 6.5. These findings help explain the absence of gel formation in MP at 10% concentration under neutral pH conditions.<sup>62–64</sup>

Based on these results, a 10% (w/w) protein concentration was selected to ensure gel formation for subsequent rheological analyses, for further investigation of gelation kinetics in NP gels, in comparison with SP and MP.

**3.7.2 Gelation kinetics of heat-induced gels.** Following the determination of NP's least gelation concentration (LGC), further experiments were conducted to investigate how NP gels developed during a controlled heating process (25 °C to 95 °C), followed by cooling (95 °C to 25 °C), as shown in Fig. 9. The gelation behaviour was monitored by measuring the storage

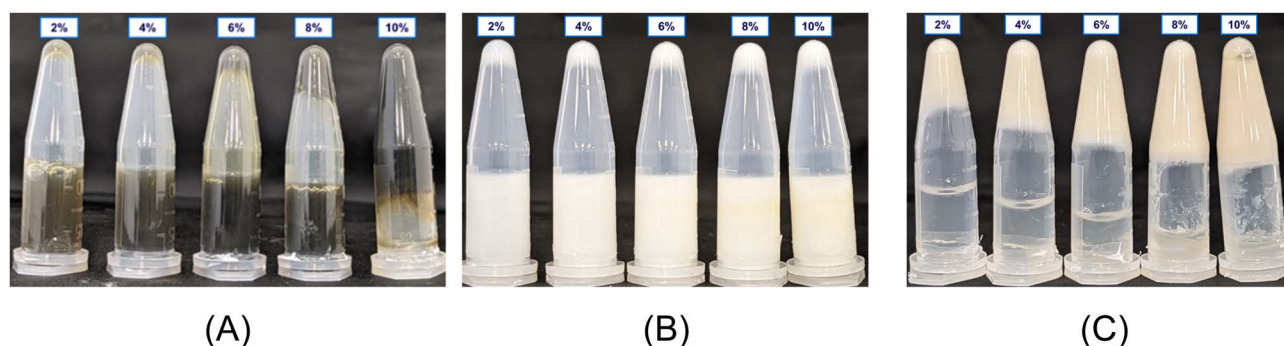


Fig. 8 Heat-induced gel formation of (A) *Nannochloropsis oceanica* protein, (B) milk protein and (C) soybean protein at different protein concentrations from 2–10% (w/w).



modulus ( $G'$ ) and loss modulus ( $G''$ ) as functions of temperature. All samples showed a progressive increase in both  $G'$  and  $G''$  during heating and cooling. Notably,  $G'$  began to exceed  $G''$  during heating and remained dominant during cooling, indicating the formation of viscoelastic solids, a hallmark of gel formation ( $G' > G''$ ). As illustrated in Fig. 9 (inset graph), the onset of gelation was closely associated with the denaturation temperature of NP, with  $G'$  starting to rise at approximately 71 °C, corresponding to the measured  $T_d$ . The thermal gelation process of NP could be divided into three distinct stages:

1. Denaturation phase: as the temperature approached 70–74 °C, the native NP proteins denatured, exposing reactive groups such as hydrophobic and thiol moieties.

2. Aggregation and network formation: in this stage, disulfide bond formation between denatured protein molecules enhances protein–protein interactions, leading to aggregation and the stabilisation of a gel network. This was reflected in a rise in both  $G'$  and  $G''$ , reaching approximately 6 Pa and 3.5 Pa, respectively.

3. Cooling and network stabilisation: during cooling from 95 °C to 25 °C (Fig. 9),  $G'$  and  $G''$  continued to increase. This behaviour suggests the formation of additional protein cross-links, likely through hydrogen bonding, which contributed to the development of a stable three-dimensional gel matrix and increased gel elasticity.

The gelation behaviour of MP and SP was also examined to compare their performance with that of NP. MP did not show gel-like characteristics at its 10% (w/w) concentration, as evidenced by the lack of change in  $G'$  and  $G''$  during the heating and cooling cycles—an observation consistent with previous findings by Garcia *et al.*<sup>65</sup> In contrast, heat-induced SP gels exhibited a clear gel-like response, marked by a significant increase in  $G'$  during heating. However, during cooling, the  $G'$  of SP gels remained lower than that of NP gels. For example, the  $G'$  value of NP at 25 °C was approximately twice that of the SP gel, indicating a more solid-like and stronger gel structure (Fig. 10).

After the heating and cooling profile, a strain sweep was conducted to examine the linear viscoelastic region and breakdown behaviour of NP and SP gels. As shown in Fig. 11,  $G'$  for NP gels gradually decreased as strain increased from 0.001 to 1, indicating a relatively narrow linear viscoelastic region. Compared to SP gels, NP gels exhibited a more brittle nature and were prone to earlier structural breakdown. Fig. 11 further illustrates this behaviour, highlighting the earlier failure of NP gels relative to SP gels. This behaviour indicates that NP gels have a weaker or less cohesive network, making them more prone to breakdown under applied strain compared to SP gels. Similar observations have been made for weak heat-induced gels formed by proteins derived from *Arthrospira platensis*, *Chlorella sorokiniana*, and *Tetraselmis suecica*, which also exhibited limited network strength under strain.<sup>58,66,67</sup>

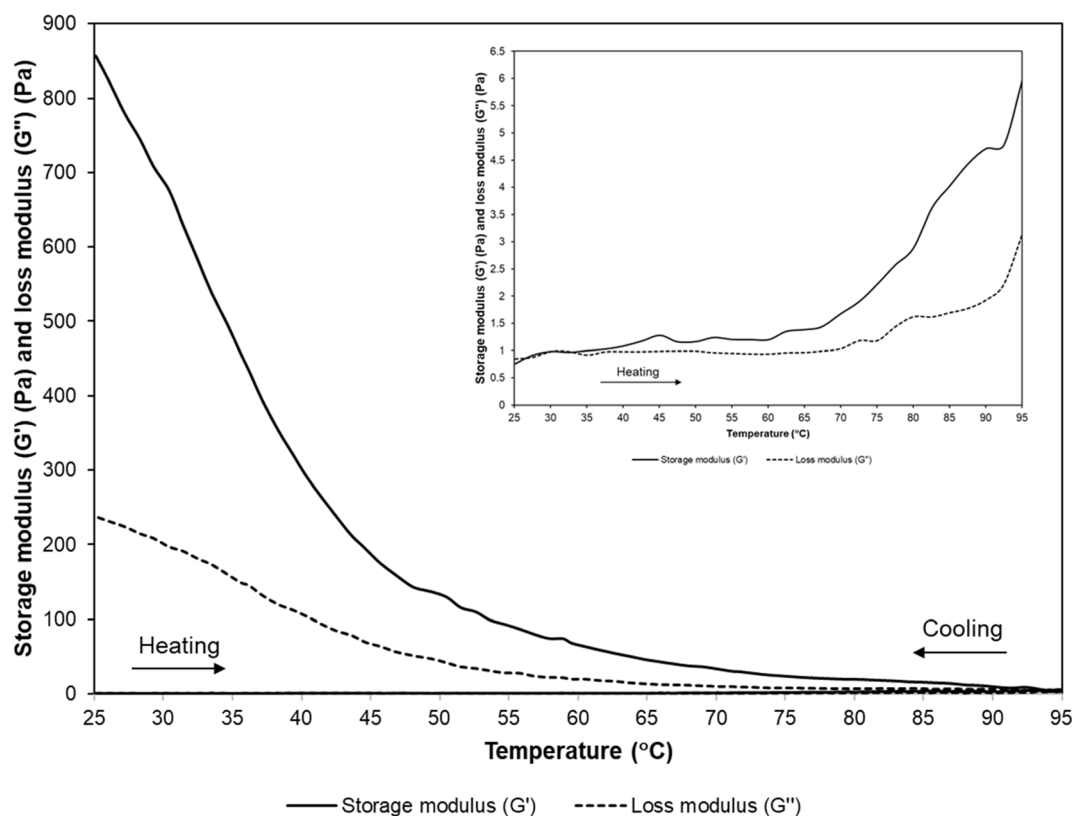


Fig. 9 Storage modulus  $G'$  (Pa) (solid line) and loss modulus  $G''$  (Pa) (dash line) as a function of temperature during heating and cooling profile of 10% (w/w) of heat-induced *Nannochloropsis oceanica* protein gels. The inset highlights increase in  $G'$  indicates the onset of gelation during heating.



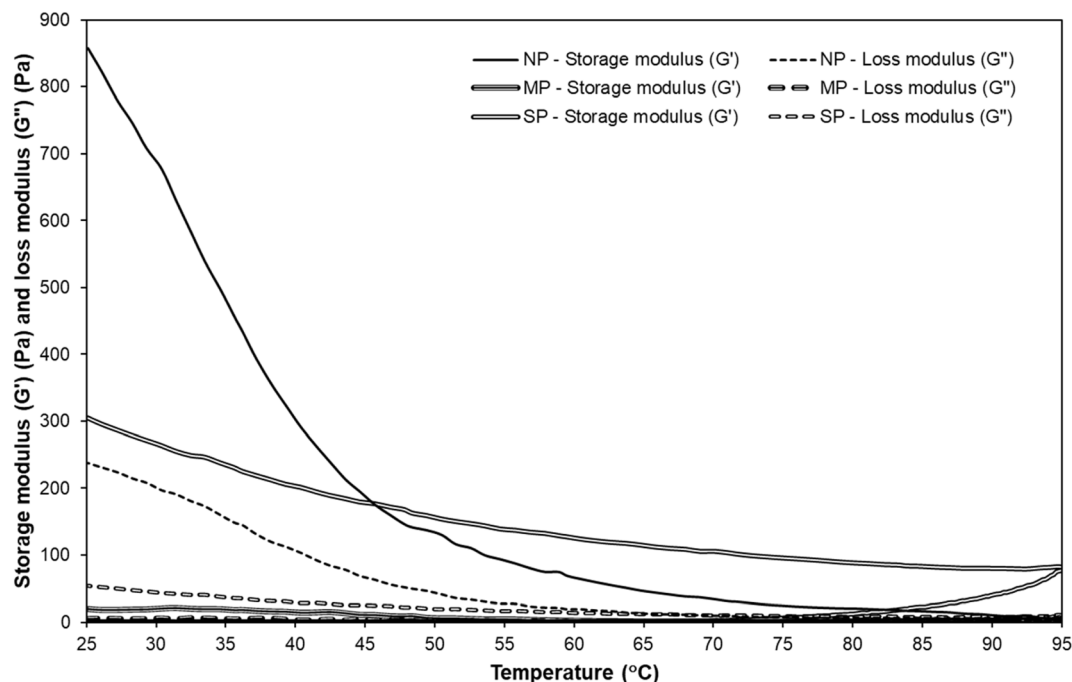


Fig. 10 Comparison of storage modulus  $G'$  (Pa) and loss modulus  $G''$  (Pa) as a function of temperature during heating and cooling profile of 10% (w/w) of three heat-induced protein gels. NP – *Nannochloropsis oceanica* protein, MP – Milk protein, and SP – Soybean protein.

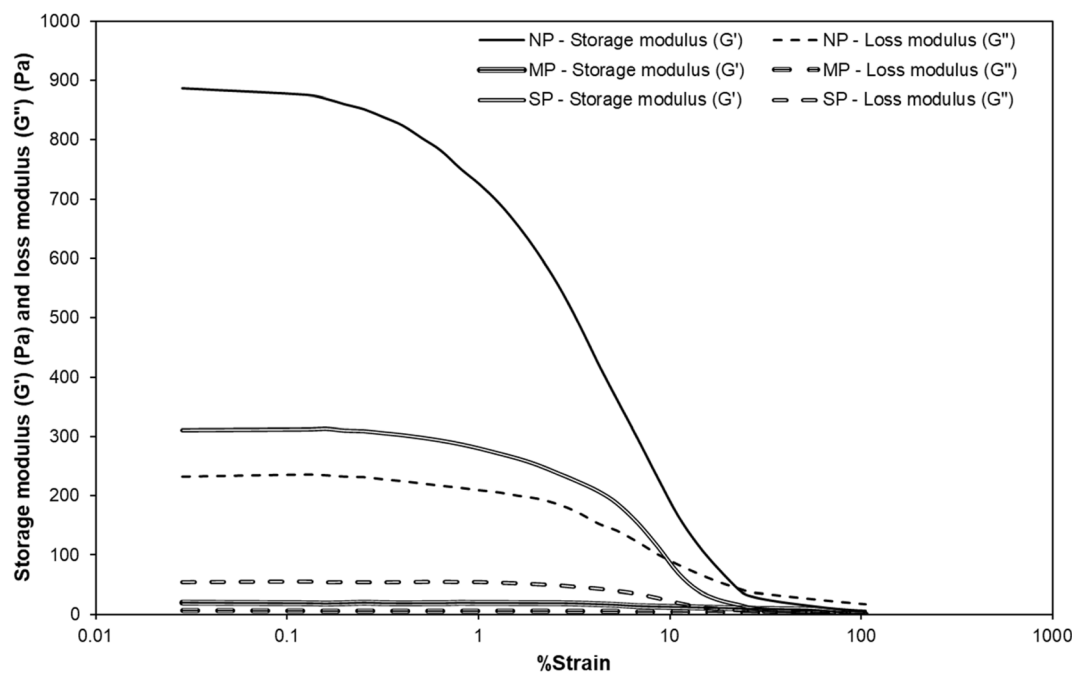


Fig. 11 Comparison of storage modulus  $G'$  (Pa) and loss modulus  $G''$  (Pa) under strain sweep from 0.1 to 100% of 10% (w/w) of three heat-induced protein gels. NP – *Nannochloropsis oceanica* protein, MP – Milk protein, and SP – Soybean protein.

## 4 Conclusion

Protein extracted from defatted *Nannochloropsis oceanica* biomass showed a high purity of 86% and demonstrated promising techno-functional properties. The *N. oceanica*

protein (NP) exhibited high surface charge density across a broad pH range (4.0–12.0), suggesting good colloidal stability in diverse food systems. Its water-absorption capacity was comparable to that of milk protein (MP) and soybean protein (SP), while its oil-absorption capacity was superior to both. The



onset and peak denaturation temperatures of NP were 68.4 °C and 71.0 °C, respectively, indicating good thermal stability. NP-stabilised oil-in-water emulsions were most effective at 1% (w/w) protein concentration and remained stable for up to 120 days, outperforming emulsions stabilised by MP and SP. NP also exhibited gel-forming ability at a minimum concentration of 10% (w/w). While the resulting heat-induced gels were elastic, they were mechanically weaker than those formed by SP. MP failed to form a gel at this concentration. Overall, these findings demonstrate that NP possesses versatile and favourable techno-functional properties, making it a strong candidate for incorporation into a variety of food formulations, including emulsified products and plant-based or alternative protein gels. Further characterisation of the chemical properties of *Nannochloropsis oceanica* proteins is recommended to deepen understanding of their structural diversity, and underlying molecular mechanisms. Such analyses could provide valuable insights into their functional roles in foaming, emulsification, water and oil absorption, thermal stability, and gelation.

## Author contributions

Thi Phuong Linh Le: conceptualisation, methodology, writing – original draft. Jayani Samarathunga: conceptualisation, writing – review and editing. Katrina Strazdins: conceptualisation, supervision, review and editing. Jeroen Rens: conceptualisation, supervision, review and editing. Benu Adhikari: conceptualisation, supervision, writing – review and editing.

## Conflicts of interest

There are no conflicts to declare.

## Data availability

The manuscript contains all data necessary to support the findings, statements, and conclusions. Any data taken from literature, if applicable, has been appropriately acknowledged and cited.

## Acknowledgements

The authors are grateful to the Bega Group of Companies for the contribution through scholarship support. We acknowledge Qponics Limited (Queensland, Australia) for providing the freeze-dried *Nannochloropsis oceanica* used in this research. We also acknowledge technical support from the Technician of Food Research and Innovation at RMIT University.

## References

- L. B. Safdar, M. J. Foulkes, F. H. Kleiner, I. R. Searle, R. A. Bhosale, I. D. Fisk and S. A. Boden, *Plant Commun.*, 2023, **4**(6), 100716.
- H. Onyeaka, T. Miri, K. Obileke, A. Hart, C. Anumudu and Z. T. Al-Sharif, *Carbon Capture Sci. Technol.*, 2021, **1**, 100007.
- A. K. Koyande, K. W. Chew, K. Rambabu, Y. Tao, D.-T. Chu and P.-L. Show, *Food Sci. Hum. Wellness*, 2019, **8**, 16–24.
- Y. Ye, M. Liu, L. Yu, H. Sun and J. Liu, *Mar. Drugs*, 2024, **22**, 54.
- R. Du Preez, M. E. Majzoub, T. Thomas, S. K. Panchal and L. Brown, *Nutrients*, 2021, **13**, 3991.
- Y. Xu, *J. Agric. Food Chem.*, 2022, **70**, 11500–11509.
- W. J. C. Sow and J. Du, *Ultrason. Sonochem.*, 2024, **105**, 106851.
- Y. Chen, J. Chen, C. Chang, J. Chen, F. Cao, J. Zhao, Y. Zheng and J. Zhu, *Food Hydrocolloids*, 2019, **96**, 510–517.
- T. P. L. Le, J. Samarathunga, M. Gabard, K. Strazdins, J. Rens and B. Adhikari, *Sustainable Food Technol.*, 2025, **3**, 549–558.
- AOAC, *Official Methods*, Gaithersburg, MD, USA, 2005.
- L. B. Pham, B. Wang, B. Zisu and B. Adhikari, *Food Hydrocolloids*, 2019, **94**, 20–29.
- H. Tomotake, I. Shimaoka, J. Kayashita, M. Nakajoh and N. Kato, *J. Agric. Food Chem.*, 2002, **50**, 2125–2129.
- Z. Zhang, G. Holden, B. Wang and B. Adhikari, *Food Chem.*, 2023, **406**, 134931.
- K. N. Pearce and J. E. Kinsella, *J. Agric. Food Chem.*, 1978, **26**, 716–723.
- K. K. Ma, L. Grossmann, A. A. Nolden, D. J. McClements and A. J. Kinchla, *Future Foods*, 2022, **6**, 100155.
- Y. Zhang, J. Zhang, Q. Chen, N. He and Q. Wang, *Foods*, 2022, **11**, 1397.
- S. Benelhadj, A. Gharsallaoui, P. Degraeve, H. Attia and D. Ghorbel, *Food Chem.*, 2016, **194**, 1056–1063.
- Y. Wang, L. Zhu, Z. Zhu, M. Liu and X. Zhao, *Molecules*, 2024, **29**, 3139.
- M. A. Devi, G. Subbulakshmi, K. M. Devi and L. Venkataraman, *J. Agric. Food Chem.*, 1981, **29**, 522–525.
- N. Boukhari, A. Doumandji and A. Ferradji, *Med. J. Nutr. Metab.*, 2018, **11**, 235–249.
- Y. Ladjal-Ettoumi, L. H. Douik, M. Hamadi, J. A. A. Abdullah, Z. Cherifi, M. N. Keddar, M. Zidour and A. Nazir, *Food Biophys.*, 2024, **19**, 439–452.
- A. M. Pereira, C. R. Lisboa and J. A. V. Costa, *Innovative Food Sci. Emerging Technol.*, 2018, **47**, 187–194.
- Q. Tang, Y. H. Roos and S. Miao, *Foods*, 2023, **12**, 368.
- O. K. Mosibo, G. Ferrentino and C. C. Udenigwe, *Foods*, 2024, **13**, 733.
- L. Böcker, P. Bertsch, D. Wenner, S. Teixeira, J. Bergfreund, S. Eder, P. Fischer and A. Mathys, *J. Colloid Interface Sci.*, 2021, **584**, 344–353.
- M. K. Ryan, R. S. Varad, M. Nicole, C. N. Pace and J. M. Scholtz, *Biophys. J.*, 2012, **102**, 1907–1915.
- L. Grossmann, J. Hinrichs and J. Weiss, *LWT–Food Sci. Technol.*, 2019, **105**, 408–416.
- S. C. Silva, T. Almeida, G. Colucci, A. Santamaria-Echart, Y. A. Manrique, M. M. Dias, L. Barros, Â. Fernandes, E. Colla and M. F. Barreiro, *Colloids Surf., A*, 2022, **648**, 129264.
- S. Bleakley and M. Hayes, *Appl. Sci.*, 2021, **11**, 3964.
- A. Taraszkiwicz, I. Sinkiewicz, A. Sommer, B. Kusznierowicz, L. Giblin and H. Staroszczyk, *Food Chem.*, 2025, **472**, 142641.



- 31 S. Belyakov, M. Voigtmann, K. Y. Win, C. Lee, D. Lee, M. N. Antipina, R. Y. M. Teo, L. W. Khoo, Y. Kanagasundaram and C. T. Busran, *ACS Food Sci. Technol.*, 2024, **4**(9), 2058–2068.
- 32 P. Kaushik, K. Dowling, S. McKnight, C. J. Barrow, B. Wang and B. Adhikari, *Food Chem.*, 2016, **197**, 212–220.
- 33 T. S. Purdi, A. D. Setiowati and A. Ningrum, *J. Food Meas. Charact.*, 2023, **17**, 5474–5486.
- 34 Z. Akbarbaglu, A. Ayaseh, B. Ghanbarzadeh and K. Sarabandi, *Algal Res.*, 2022, **66**, 102755.
- 35 L. Mauer, in *Encyclopedia of Food Sciences and Nutrition*, ed. B. Caballero, Academic Press, Oxford, 2nd edn, 2003, pp. 4868–4872, DOI: [10.1016/B0-12-227055-X/00988-3](https://doi.org/10.1016/B0-12-227055-X/00988-3).
- 36 E. Taragjini, M. Ciardi, E. Musari, S. Villaró, A. Morillas-España, F. J. Alarcón and T. Lafarga, *Food Bioprocess Technol.*, 2022, **15**, 1299–1310.
- 37 S. Wu, P. Menut, S. Miao and C. Turchiuli, *Compr. Rev. Food Sci. Food Saf.*, 2025, **24**, e70264.
- 38 P. Moll, H. Salminen, E. Griesshaber, C. Schmitt and J. Weiss, *J. Food Sci.*, 2022, **87**, 4622–4635.
- 39 S. Sai-Ut, S. Ketnawa, P. Chaiwut and S. Rawdkuen, *Asian Journal of Food and Agro-Industry*, 2009, **2**, 493–504.
- 40 M. Ozgolet, Z. H. T. Cakmak, F. Bozkurt, O. Sagdic and S. Karasu, *Food Sci. Nutr.*, 2024, **12**, 3346–3359.
- 41 Y. Wen, X. Dong, L. N. Zamora, A. G. Jeffs and S. Y. Quek, *Foods*, 2024, **13**, 2735.
- 42 A. Cano-Medina, H. Jiménez-Islas, L. Dendooven, R. P. Herrera, G. González-Alatorre and E. M. Escamilla-Silva, *Food Res. Int.*, 2011, **44**, 684–692.
- 43 M. Joshi, B. Adhikari, P. Aldred, J. Panozzo, S. Kasapis and C. Barrow, *Food Chem.*, 2012, **134**, 1343–1353.
- 44 W. Liang, F. Deng, Y. Wang, W. Yue, D. Hu, J. Rong, R. Liu, S. Xiong and Y. Hu, *Food Hydrocolloids*, 2024, **149**, 109611.
- 45 L. Grossmann, S. Ebert, J. R. Hinrichs and J. Weiss, *J. Agric. Food Chem.*, 2019, **67**, 6551–6558.
- 46 C. Liu, F.-S. Chen, R.-H. Niu and Y.-H. Gao, *J. Oleo Sci.*, 2020, **69**, 1445–1453.
- 47 Y. Tan, P. W. Lee, T. D. Martens and D. J. McClements, *Food Biophys.*, 2022, **17**, 409–421.
- 48 C. E. Gumus, E. A. Decker and D. J. McClements, *Food Biophys.*, 2017, **12**, 186–197.
- 49 D. Li, Y. Zhao, X. Wang, H. Tang, N. Wu, F. Wu, D. Yu and W. Elfalleh, *Food Hydrocolloids*, 2020, **98**, 105306.
- 50 L. Zhou, I. Ali, S. Manickam, B. H. Goh, Y. Tao, J. Zhang, S. Y. Tang and W. Zhang, *Compr. Rev. Food Sci. Food Saf.*, 2025, **24**, e70162.
- 51 L. Zheng, J. M. Regenstein, L. Zhou and Z. Wang, *Compr. Rev. Food Sci. Food Saf.*, 2022, **21**, 1940–1957.
- 52 G. Karabulut, H. Feng and O. Yemiş, *Plant Foods Hum. Nutr.*, 2022, **77**, 577–583.
- 53 M. A. Haque, P. Aldred, J. Chen, C. J. Barrow and B. Adhikari, *Food Chem.*, 2013, **141**, 702–711.
- 54 S. Van De Walle, I. Gifuni, B. Coleman, M.-C. Baune, A. Rodrigues, H. Cardoso, F. Fanari, K. Muylaert and G. Van Royen, *Food Res. Int.*, 2024, **182**, 114142.
- 55 Z. Zhang, B. Wang, G. Holden, J. Chen and B. Adhikari, *Future Foods*, 2023, **7**, 100239.
- 56 C. Moreira, P. Ferreira-Santos, R. Nunes, B. Carvalho, H. Pereira, J. A. Teixeira and C. M. Rocha, *Algal Res.*, 2025, **86**, 103958.
- 57 J.-L. Maubois and D. Lorient, *Dairy Sci. Technol.*, 2016, **96**, 15–25.
- 58 L. Grossmann, J. Hinrichs, H. D. Goff and J. Weiss, *Innovative Food Sci. Emerging Technol.*, 2019, **56**, 102176.
- 59 Y. Ma, S. Fu, K.-W. Cheng and B. Liu, *Int. J. Biol. Macromol.*, 2025, **286**, 138363.
- 60 I. S. Chronakis, *J. Agric. Food Chem.*, 2001, **49**, 888–898.
- 61 B. Guldiken, J. Stobbs and M. Nickerson, *Food Chem.*, 2021, **350**, 129158.
- 62 P. Thomar and T. Nicolai, *Colloids Surf., B*, 2016, **146**, 801–807.
- 63 A. Kharlamova, T. Nicolai and C. Chassenieux, *Food Hydrocolloids*, 2019, **92**, 198–207.
- 64 T. Nicolai and C. Chassenieux, *Food Hydrocolloids*, 2021, **118**, 106755.
- 65 E. S. Garcia, J. Van Leeuwen, C. Safi, L. Sijtsma, L. A. van den Broek, M. H. Eppink, R. H. Wijffels and C. van den Berg, *J. Agric. Food Chem.*, 2018, **66**, 7831–7838.
- 66 H. S. Lozober, Z. Okun and A. Shpigelman, *Innovative Food Sci. Emerging Technol.*, 2021, **74**, 102857.
- 67 E. S. Garcia, J. Van Leeuwen, C. Safi, L. Sijtsma, M. H. Eppink, R. H. Wijffels and C. van den Berg, *Bioresour. Technol.*, 2018, **268**, 197–203.

